



**Grant agreement no. 201076**

**nEUROPt**

**Non-invasive imaging of brain function and disease by pulsed near infrared light**

***Collaborative project (Small or medium-scale focused research project)***

**Objective HEALTH-2007-1.2-2**

**Novel optical methodologies for detection, diagnosis and monitoring of disease or disease-related processes**

**Final report**

**WP5 attachments**

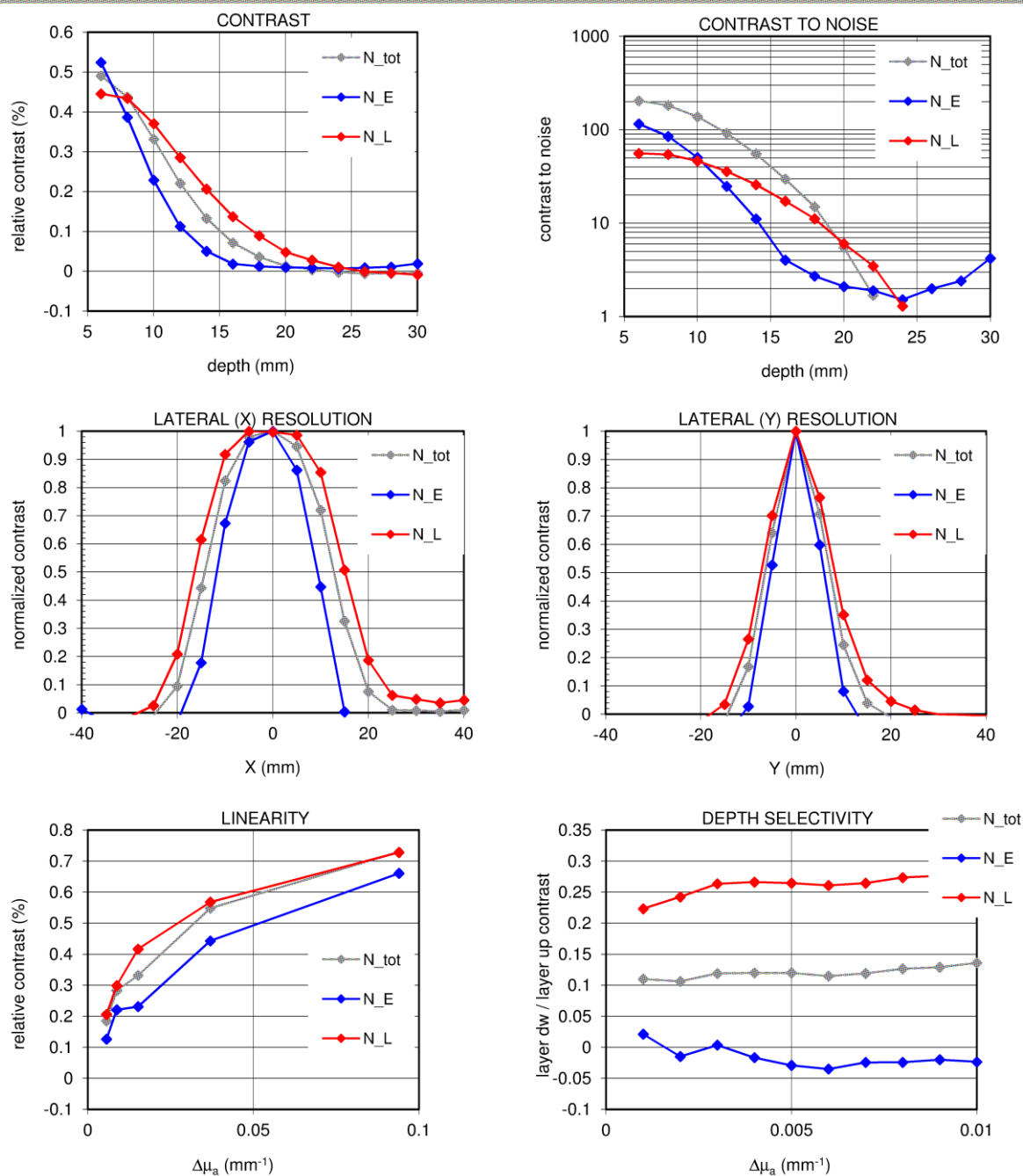
Table 5.1. Instruments and configurations characterized.

Partner	PoliMi FIS	PoliMi FIS	IBIB	UCL MPB	PTB	PTB	PTB	PTB
Instrument / configuration acronym	fOXY	DiffS		MONSTIR II	PTB_1	PTB_2	PTB_3	PTB_4
Letter code	A	F	B		D	E		G
Instrument name	PoliMi brain imager	PoliMi lab setup	IBIB brain imager	UCL brain imager	PTB brain imager			PTB lab setup
_ reference paper	Contini OE 2006		Kacprzak JBO 2007		Wabnitz SPIE 2005			
<b>Source</b>								
_ kind	diode laser	supercontinuum laser + prism	ps diode laser	supercontinuum laser + AOTF	ps diode laser			supercontinuum laser with AOTF
_ type	PDL 800 (LDH-635,	SC400	Sepia II	SC400	Sepia II			SC500-6-custom
_ manufacturer	Picoquant	Fianium	Picoquant	Fianium	Picoquant			Fianium
_ wavelength(s) / nm	690,820		687, 750, 832		690, 800, 830			
<b>Detector</b>								
_ type	R5900U-20-M4 (multialkali)	R1564U-S1 (MultiChannel Plate)	R7400U-02	H8422-P50	R7400U-02	H7422-50	HPM-100-50	HPM-100-50
_ cathode	Multialkali	multialkali	multialkali	GaAs	multialkali	GaAs	GaAs	GaAs
_ manufacturer	Hamamatsu	Hamamatsu	Hamamatsu	Hamamatsu	Hamamatsu	Hamamatsu	Becker&Hickl	Becker&Hickl
_ cooled (Y/N)	Y	Y	N	Y	N	Y	N	N
_ remarks					imager module with variable attenuation (diaphragm) and NA (diaphragm)	imager module with variable attenuation (filter wheel) and NA (diaphragm)	combined with lab setup	lab setup
<b>Source fiber</b>								
_ diameter / mm	0.1	0.05	0.4	0.0625	0.2	0.2	0.2	0.062 (GIF)
_ length / m	3	2	2	3	2	2	2	2
_ NA	0.29	0.21	0.39	0.25	0.39	0.39	0.39	0.275
_ remarks							tip painted black	tip painted black
<b>Detection fiber / bundle</b>								
_ diameter / mm	3	1	4	3	4	4	1	1
_ length / m	1.5	1	1.5	3	1.5	1.5	2	2
_ NA	0.49	0.39	0.54	0.45	0.54	0.54	0.39	0.39
_ remarks							tip painted black	tip painted black
<b>Protocols performed (Y/N)</b>								
BIP	Y	Y	Y	Y	Y	Y	N	N
MEDPHOT	Y	N	Y	Y	Y	Y	N	Y
nEUROpt	Y	N	Y	Y	Y	Y	Y	N

# nEUROPt PROTOCOL for Assessment of Time-Domain Optical Brain Imagers

Ver.1.1

Group POLIMI Setup FOXY Name Time-Resolved Functional Oximeter Date 30.09.11  
lambda 830 nm rho 3 cm mu\_a 0.01 mm^-1 mu\_s' 1 mm^-1 V\_o 1000 mm^3 z\_0 10 mm d 10 mm



## SYNTHETIC DESCRIPTORS

parameter	target	unit	output	unit	N_tot	N_E	N_L
contrast	15	mm	contrast		10.2%	3.4%	17.2%
CNR	10		z	mm	19.0	14.3	18.4
X-resolution	50%		resolution	mm	27	21	32
Y-resolution	50%		resolution	mm	14	11	16
depth selectivity	0.004	mm <sup>-1</sup>	selectivity		0.12	-0.02	0.27
linearity			H <sup>+</sup>		0.902	0.941	0.854

Fig. 5.1 Front page of reporting sheet for the nEUROPt protocol for an exemplary instrument (PoliMi FOXY at 830 nm) and data analysis (time windows) (from Deliverable 5.4)

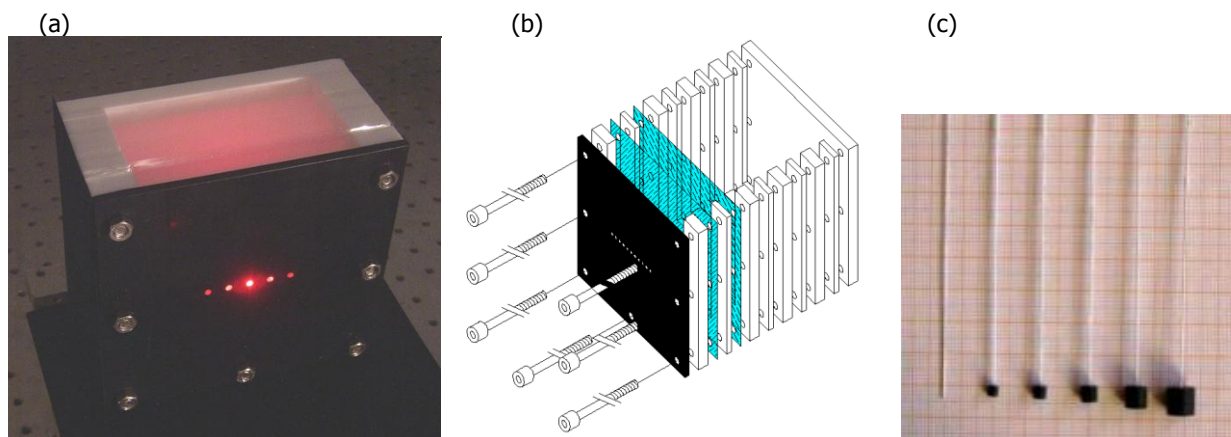


Fig. 5.2 **Liquid phantoms:** Scattering cell (a), realization of layered phantoms (with Mylar foil inserted to separate compartments) (b) and phantoms with localized inclusions (PVC cylinders of various size, with diameter = height of 3.2 mm, 4 mm, 5 mm, 6.8 mm, 8.6 mm) (c) (UniFi).

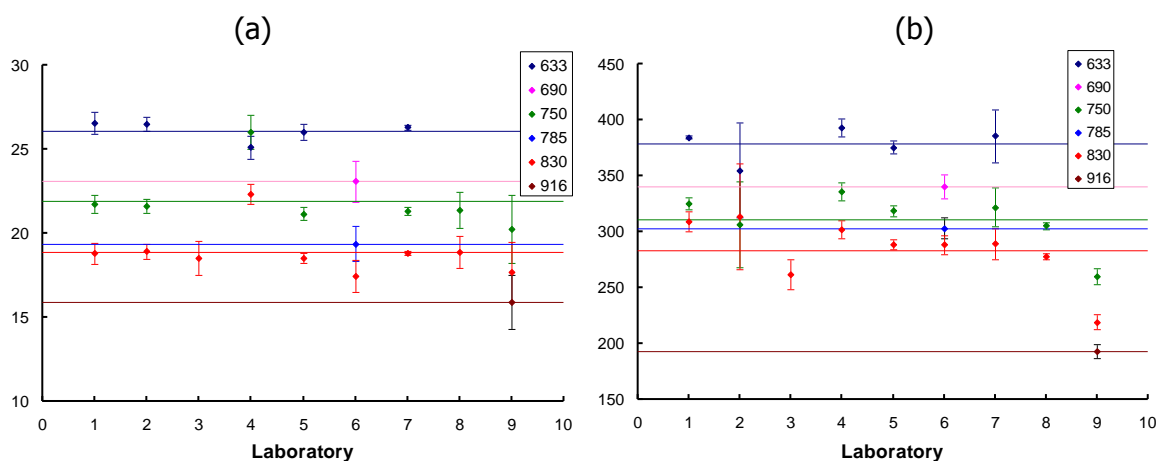


Fig. 5.3 Results of the inter-laboratory study to characterize materials for liquid phantoms [L. Spinelli et al., OSA 2012, BW1A.6]. Intrinsic reduced scattering coefficient of Intralipid (a), and intrinsic absorption coefficient of ink (b), obtained at different wavelengths (coded by colors, nm in the legend) by the 9 laboratories. Statistical uncertainties (error bars represent one standard deviation) and averages at each wavelengths (straight lines) are also reported.



Fig. 5.4 **Responsivity phantom** (PTB). For characterization of the phantoms see [H. Wabnitz et al., Proc. SPIE 7896 (2011), 789602].

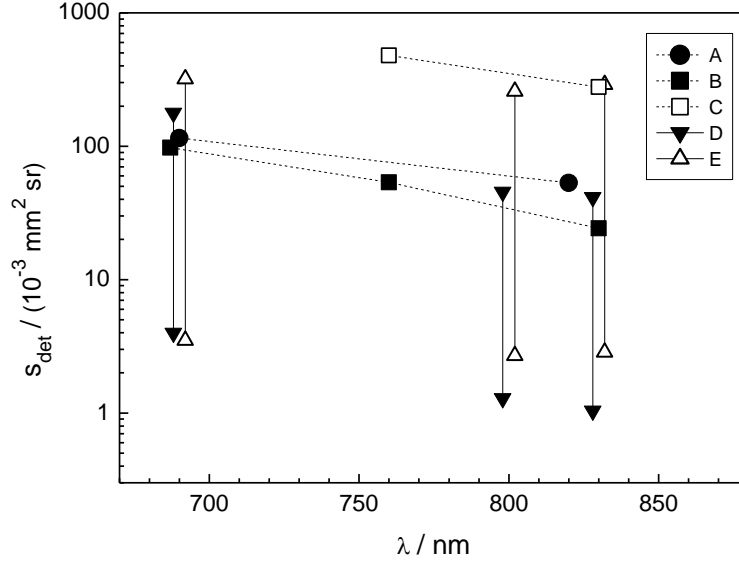


Fig. 5.5 **Responsivity**  $S_{\text{det}}$  of the detection system as a function of wavelength measured for various instruments of PoliMi\_FIS, PTB and IBIB (letter codes see Table 5.1). The ranges marked by vertical lines for A and E pertain to various settings of attenuators and effective numerical aperture. A wavelength offset between D and E has been added for clarity. The responsivity measurement is described in detail in [H. Wabnitz et al., Proc. SPIE 7896 (2011), 789602]. It is interesting to note that all brain imagers compared (instruments A, B, D) have very similar responsivity values  $S_{\text{det}}$ , differing by a factor of 2 at most, in spite of using different photomultipliers, fiber bundles and optical systems.

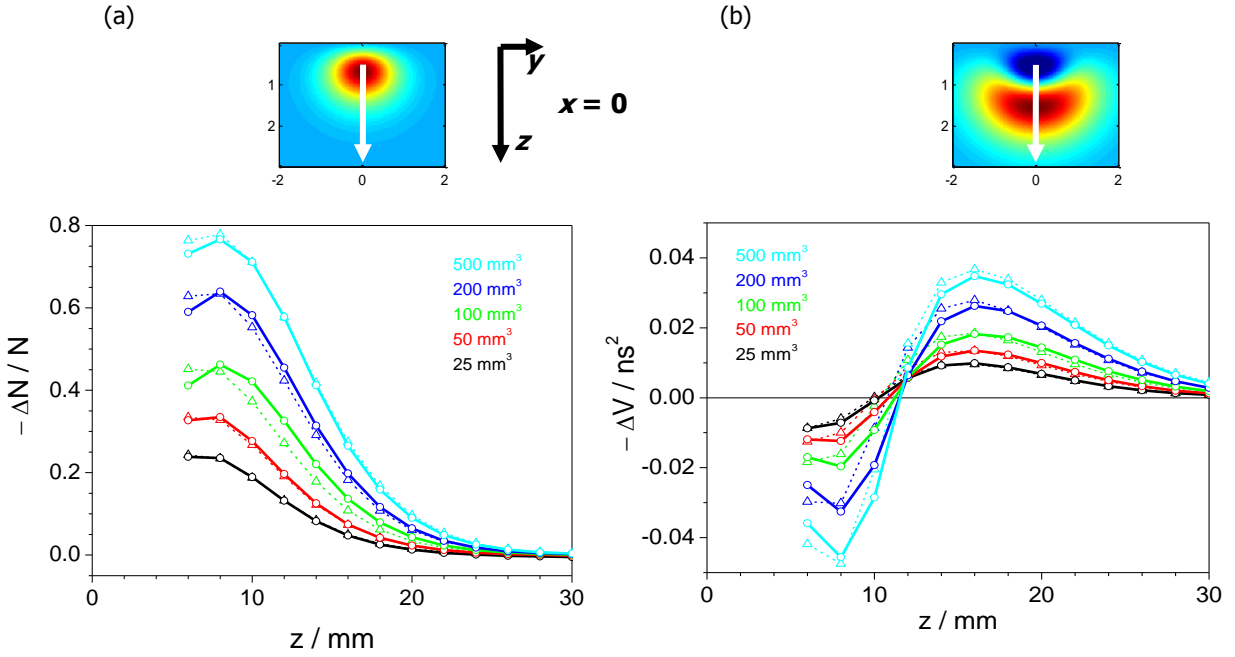


Fig. 5.6 **z scans** of black PVC cylinders: Relative contrast for total photon count  $N$  (a) and difference in variance (b), circles – experiment with configuration PTB3, triangles – MC simulation (UniFi). The agreement between measurements and experiment is very good. Above the graphs, the sensitivities to point-like absorbing perturbations are shown for a source-detector separation of 3 cm, in the midplane between source and detector, dimensions in cm. White arrows represent the  $z$  scan.

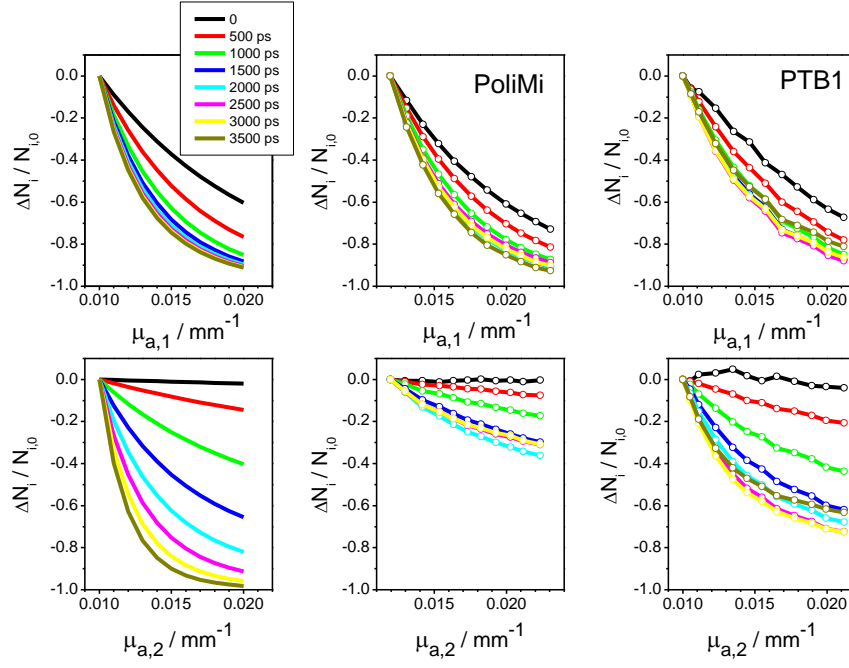


Fig. 5.7 **Two-layer measurements** for determination of depth selectivity: Contrasts (PoliMi\_FIS and PTB1) of time windows of 500 ps width (left limit given in the legend) as a function of a change in  $\mu_{a,1}$  in the upper layer (upper row) and  $\mu_{a,2}$  in the lower layer (bottom row). Left column: 2-layer simulation with thickness of upper layer  $d = 10$  mm.

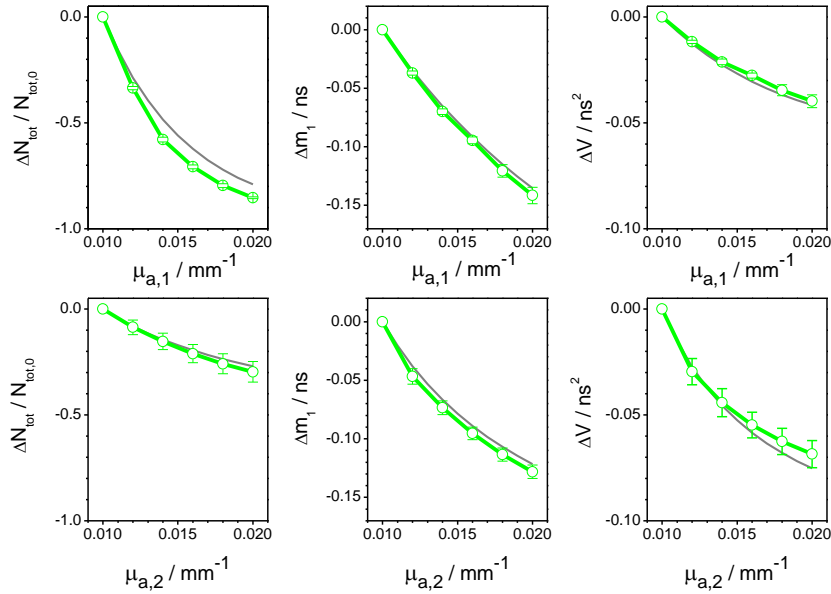


Fig. 5.8 **Two-layer measurements** for determination of depth selectivity: Contrasts (IBIB) of moments ( $N_{tot}$ ,  $m_1$ ,  $V$ ) as a function of a change in  $\mu_{a,1}$  in the upper layer (top row) and  $\mu_{a,2}$  in the lower layer (bottom row). Both integration limits for moments were set at 1% of the maximum. Grey line: 2-layer simulation with thickness of upper layer  $d = 10$  mm. In general, the  $N_{tot}$  contrast is larger in the upper layer (by about a factor of 2), for  $m_1$  it is approximately the same in both layers, whereas the sensitivity of  $V$  is larger (by about a factor of 2) for absorption changes in the lower layer.

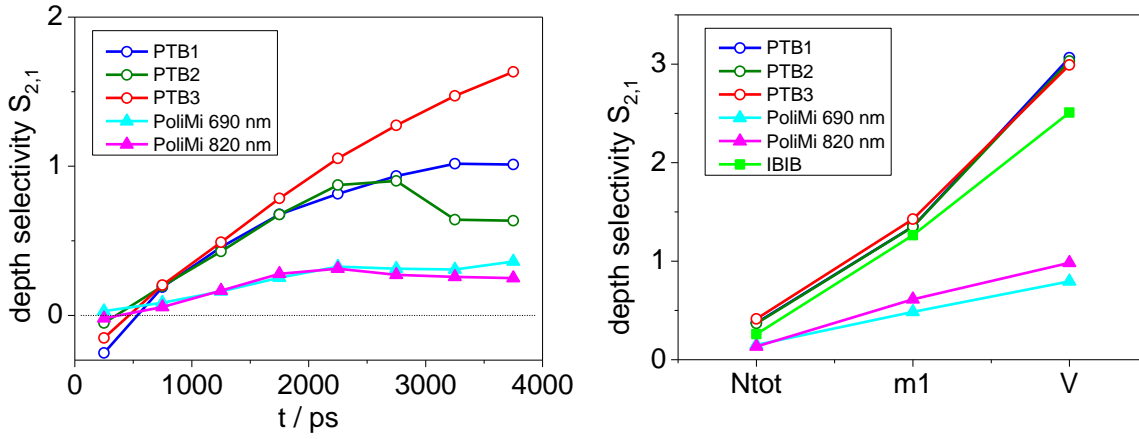


Fig. 5.9 **Depth selectivity**, i.e. the ratio of contrasts for an absorption change in the lower layer and that in the upper layer, for time windows (a) and moments (b). The results for moments are rather consistent and independent of the IRF whereas the results for time windows reveal the influence of the IRF. The highest depth selectivity (approx. 3) is obtained for variance. Discrepancies between measurements by different partners may be due to inaccuracies in the thickness of the upper layer caused by the difficulty to accurately position the Mylar foil that separates both layers.

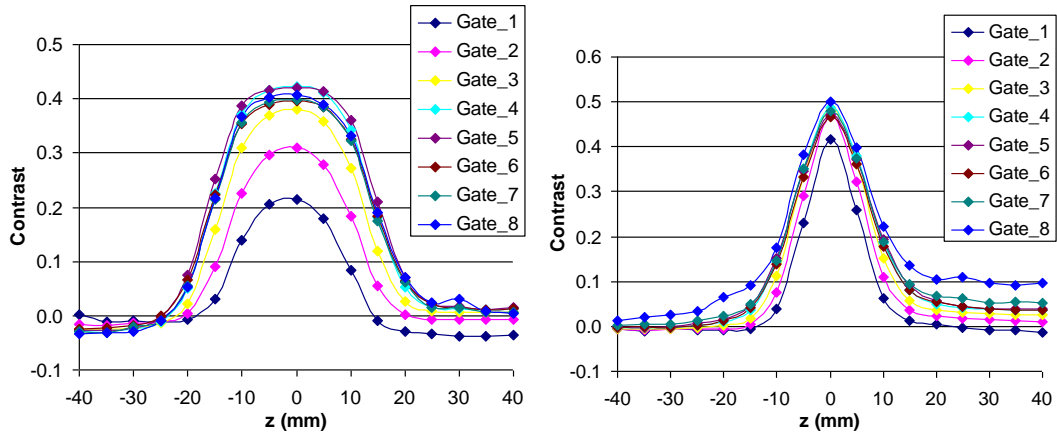


Fig. 5.10 **Lateral spatial resolution**: Contrast  $-\Delta N_i/N_i$  for an x scan (a) and a y scan (b) for various time windows for the PoliMi\_FIS brain imager (A) at 690 nm. Gate\_1, Gate\_2 etc. represent the time windows 0...500 ps, 500 ps...1000 ps etc.